Laser and Particle Beams (2015), *33*, 299–305.
©Cambridge University Press, 2015 0263-0346/15
doi:10.1017/S0263034615000191

Laser-assisted proton collision on light nuclei at moderate energies

I.F. BARNA[1,2] AND S. VARRÓ[1,2]
[1]Wigner Research Centre of the Hungarian Academy of Sciences, Budapest, Hungary
[2]ELI-HU Nonprofit Kft., Szeged, Hungary

(Received 26 September 2014; Accepted 9 February 2015)

Abstract

We present a non-relativistic analytic quantum mechanical model to calculate angular differential cross-sections for laser-assisted proton nucleon scattering on a Woods–Saxon optical potential where the *n*th-order photon absorption is taken into account simultaneously. With this novel description we can integrate two well-established fields, namely low-energy nuclear physics and multi-photon processes together. As a physical example we calculate cross-sections for proton–^{12}C collision at 49 MeV in the laboratory frame in various realistic laser fields. We consider optical Ti:sapphire and X-ray lasers with intensities which are available in existing laser facilities or in the future ELI or X-FEL.

Keywords: Inelastic proton scattering; Optical potential; Other multi-photon processes

1. INTRODUCTION

Nowadays optical laser intensities exceeded the 10^{22} W/cm^2 limit where radiation effects dominate the electron dynamics. In the field of laser–matter interaction a large number of non-linear response of atoms, molecules, and plasmas can be investigated both theoretically and experimentally. Such interesting high-field phenomena are high harmonic generations, or plasma-based laser-electron acceleration. These field intensities open the door to high-field quantum electrodynamics phenomena like vacuum-polarization effects of pair production (Di Piazza *et al.*, 2012). In most of the presented studies the dynamics of the participating electrons are investigated. Numerous surveys on laser-assisted electron collisions are available such as Ehlotzky *et al.* (1998). However, there are only few nuclear photo-excitation investigations done where some low-lying first excited states of medium of heavy elements are populated with the help of X-ray free-electron laser pulses (Gunst *et al.*, 2014). Nuclear excitation by atomic electron re-scattering in a laser field was investigated by Kornev and Zon (2007). Various additional concepts are under consideration for photo-nuclear reactions by laser-driven gamma beams (Habs *et al.*, 2009). Some applications of laser-induced nuclear physics can be found in the study of Ledingham (2005).

To our knowledge there are no publications available where laser-assisted proton nucleus collisions (or radiative proton–nucleus scattering) were investigated. This is the goal of our recent paper. We consider the global optical potential of Woods and Saxon (1954) (WS) with the proper parameterization for moderate energy proton–^{12}C collision (Abdul-Jalil & Jackson, 1979). The optical potential formalism has been a very successful method to study the single-particle spectra of nucleus in the last five decades. Detailed description and the validity of this formalism can be found in nuclear physics textbooks or in monographs like von Geramb (1979); Varner *et al.*, (1991); Hodgson (1994); Greiner and Maruhn (1996).

The nuclear physics community recently managed to evaluate the closed analytic form of the Fourier transformed WS interaction (Hlophe *et al.*, 2013) which is a great success. Former time only an analytic series function was available to approximate the WS potentials (Pahlavani & Morad, 2010).

We incorporate these results into a first Born approximation scattering cross-section formula where the initial and final proton wave functions are Volkov waves and the induced photon emission and absorption processes are taken into account up to arbitrary orders (Bunkin & Fedorov, 1965; Bunkin *et al.*, 1973; Faisal 1973; 1987; Kroll & Watson, 1973; Gontier & Rahman, 1974; Bergou, 1980;

Address correspondence and reprint requests to: I. F. Barna, Wigner Research Centre of the Hungarian Academy of Sciences, Konkoly Thege Miklós út 29-33, 1121 Budapest, Hungary. E-mail: barna.imre@wigner.mta.hu

Bergou & Varró, 1980). This kind of multi-photon description was very successful in the last four decades and helped to understand various optical and physical phenomena.

We hope that our description will open a new path in the field of photo-nuclear studies in the near future. For a better understanding we end our study with two physical examples where 49 MeV protons are scattered on ^{12}C nuclei in various laser fields. At first we consider the field of a Ti:sapphire laser which has optical frequency with intensities even 10^{22} W/cm^2. As a second case we present calculations for X-ray lasers which have much larger photon energy but much lower intensity available at the time.

2. THEORY

In the following, we summarize our applied non-relativistic quantum mechanical description. The laser field is handled in the classical way via the minimal coupling. The laser beam is taken to be linearly polarized and the dipole approximation is used. If the dimensionless intensity parameter (or the normalized vector potential) $a_0 = 8.55\times 10^{-10}\sqrt{I(\mathrm{W/cm^2})}\lambda(\mu\mathrm{m})$ of the laser field is smaller than unity the non-relativistic description in dipole approximation is valid. For 800 nm laser wavelength this means a critical intensity of $I = 2.13\times 10^{18}$ W/cm^2. In case of protons a_0 is replaced by $a_p = [(m_p/m_e)^{-1}]a_0$, where the proton to electron mass ratio is $(m_p/m_e) = 1836$. Accordingly, for 800 nm wavelength the critical intensity for protons is $I_{crit} = 3.91\times 10^{21}$ W/cm^2.

Beyond the optical regime we investigate the scattering process in an X-ray laser field as well. Typical X-ray lasers can have photon energy in the range of 1–10 keV, pulse energy of 3 mJ and 10^{12}–10^{13} photons/s photon number and the pulse duration is between 10 and 100 fs (the wavelength of a 10 keV X-ray photon is 18.2 nm). In the X-ray laser community, the photon number is the crucial parameter and not the intensity. However, the maximal achievable intensity can be calculated when the maximal focal spot is known. Focusing of X-ray laser pulses gives up numerous not trivial questions for experimentalist and still under development therefore we consider a maximal available intensity at 10^{16} W/cm^2 for a 10 keV laser pulse in our last model, where the dimensionless intensity parameter $a_0 = 1,\ 5\times 10^{-5}$. Note, that this is a small value compared to optical frequencies. The critical intensity for the 10 keV photon is a factor of 1836 times higher than for the 800 nm optical frequency.

Additionally, we consider moderate proton kinetic energy, not so much above the Coulomb barrier and neglect the interchange term between the proton projectile an the target carbon protons. This proton exchange effect could be included in the presented model with the help of Woods–Saxon potentials of non-local type (Barna *et al.*, 2000) but not in the scope of the recent study.

To describe the non-relativistic scattering process of a proton on a nucleus in a spherically symmetric external field the following Schrödinger equation has to be solved,

$$\left[\frac{1}{2m}\left(\hat{\mathbf{p}} - \frac{e}{c}\mathbf{A}\right)^2 + U(\mathbf{r})\right]\Psi = i\hbar\frac{\partial\Psi}{\partial t}, \tag{1}$$

where $\hat{\mathbf{p}} = -i\hbar\,\partial/\partial\mathbf{r}$ is the momentum operator of the proton, and $U(\mathbf{r})$ represents the scattering potential of the nucleon, $\mathbf{A}(t) = A_0\boldsymbol{\epsilon}\cos(\omega t)$ is the vector potential of the external laser field with unit polarization vector $\boldsymbol{\epsilon}$. Figure 1 presents the scattering geometry for a better understanding. The $\mathbf{p}_i$ and $\mathbf{p}_f$ are the initial and final proton momenta, θ is the scattering angle of the proton, the laser is linearly polarized in the x–z plane, and the propagation of the laser field is parallel to the x-axis.

Without the external scattering potential $U(\mathbf{r})$ the particular solution of (1) can be immediately written down as non-relativistic Volkov states $\varphi_p(\mathbf{r}, t)$ which exactly incorporate the interaction with the laser field,

$$\varphi_p(\mathbf{r}, t) = \frac{1}{(2\pi\hbar)^{3/2}}\exp\left[\frac{i}{\hbar}\mathbf{p}\cdot\mathbf{r} - \int_{t_0}^{t} dt'\,\frac{1}{2m}\left(\mathbf{p} - \frac{e}{c}\mathbf{A}(t')\right)^2\right]. \tag{2}$$

Volkov states, which are modulated de Broglie waves, parameterized by momenta $\mathbf{p}$ and form an orthonormal and complete set,

$$\int d^3r\,\varphi_p^*(\mathbf{r}, t)\varphi_{p'}(\mathbf{r}, t) = \delta_3(\mathbf{p} - \mathbf{p}'),$$
$$\int d^3p\,\varphi_p(\mathbf{r}, t)\varphi_p^*(\mathbf{r}', t) = \delta_3(\mathbf{r} - \mathbf{r}'). \tag{3}$$

To solve the original problem of Eq. (1) we write the exact wave function as a superposition of an incoming Volkov state and a correction term, which vanishes at the beginning

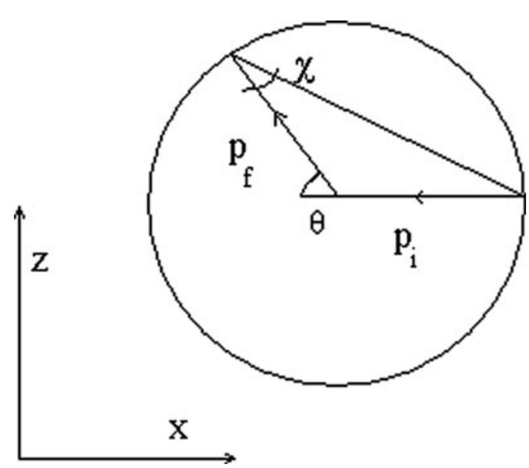

Fig. 1. The geometry of the scattering process. The ^{12}C nucleus is in the center of the circle, $\mathbf{p}_i$ and $\mathbf{p}_f$ stand for the initial and final scattered proton momenta, θ is the proton scattering angle, laser pulse propagates parallel to the x-axis and linearly polarized in the x–z plane. The χ angle is needed for the laser-proton momentum transfer.

of the interaction (in the remote past $t_0 \to -\infty$). The correction term can also be expressed in terms of the Volkov states, since these form a complete set [see the equation of (3)],

$$\Psi(\mathbf{r},t) = \varphi_{\mathrm{p_i}}(\mathbf{r},t) + \int d^3p\,a_{\mathrm{p}}(t)\varphi_{\mathrm{p}}(\mathbf{r},t), \quad a_{\mathrm{p}}(t_0) = 0. \tag{4}$$

It is clear that the unknown expansion coefficients $a_p(t)$ describe the non-trivial transition symbolized as $\mathbf{p}_i \to \mathbf{p}$, from a Volkov state of momentum $\mathbf{p}_i$ to another Volkov state with momentum $\mathbf{p}$. If we take the projection of Ψ into some Volkov state $\varphi_{\mathrm{p}}(t)$, we get

$$\int d^3r\varphi^*_{\mathrm{p}}(\mathbf{r},t)\Psi(\mathbf{r},t) = \delta_3(\mathbf{p}-\mathbf{p}_{\mathrm{i}}) + a_{\mathrm{p}}(t). \tag{5}$$

Bye inserting Ψ of Eq. (4) into the complete Schrödinger equation (1), we receive the following integro-differential equation for the coefficients $a_{\mathrm{p}}(t)$:

$$\begin{aligned} i\hbar\,\dot{a}_{\mathrm{p'}}(t) = &\int d^3r\varphi^*_{\mathrm{p'}}(\mathbf{r},t')U(\mathbf{r})\varphi_{\mathrm{p_i}}(\mathbf{r},t') \\ &+ \int d^3p\,a_{\mathrm{p}}(t)\int d^3r\varphi^*_{\mathrm{p'}}(\mathbf{r},t')U(\mathbf{r})\varphi_{\mathrm{p}}(\mathbf{r},t'), \end{aligned} \tag{6}$$

where the scalar product was taken with $\varphi_{\mathrm{p'}}(t)$ on both sides of the resulting equation and the orthogonality property of the Volkov sates was taken after all [see the first equation of (3)]. Owing to the initial condition $a_{\mathrm{p}}(t_0) = 0$, displayed already in Eq. (4) the formal solution of (6) can be written as

$$\begin{aligned} a_{\mathrm{p'}}(t) = &-\frac{i}{\hbar}\int_{t_0}^{t} dt' \int d^3r\varphi^*_{\mathrm{p'}}(\mathbf{r},t')U(\mathbf{r})\varphi_{\mathrm{p_i}}(\mathbf{r},t') \\ &-\frac{i}{\hbar}\int_{t_0}^{t} dt' \int d^3p\,a_{\mathrm{p}}(t')\int d^3r\varphi^*_{\mathrm{p'}}(\mathbf{r},t')U(\mathbf{r})\varphi_{\mathrm{p}}(\mathbf{r},t'). \end{aligned} \tag{7}$$

In the spirit of the iteration procedure used in scattering theory the $(k+1)$th iterate of $a_{\mathrm{p}}(t)$ is expresses by the kth iterate on the right-hand side in (7) like

$$\begin{aligned} a^{(k+1)}_{\mathrm{p}}(t) = &-\frac{i}{\hbar}\int_{t_0}^{t} dt' \int d^3r\varphi^*_{\mathrm{p'}}(\mathbf{r},t')U(\mathbf{r})\varphi_{\mathrm{p_i}}(\mathbf{r},t') \\ &-\frac{i}{\hbar}\int_{t_0}^{t} dt' \int d^3p\,a^{(k)}_{\mathrm{p}}(t')\int d^3r\varphi^*_{\mathrm{p'}}(\mathbf{r},t')U(\mathbf{r})\varphi_{\mathrm{p}}(\mathbf{r},t'). \end{aligned} \tag{8}$$

In the first Born approximation [where the transition amplitude is linear in the scattering potential $U(\mathbf{r})$], we receive the transition amplitude in the next form

$$\begin{aligned} T_{\mathrm{fi}} &= \lim_{t\to\infty}\lim_{t_0\to-\infty} a^{(1)}_{\mathrm{p_f}}(t) \\ &= -\frac{i}{\hbar}\int_{-\infty}^{\infty} dt' \int d^3r\varphi^*_{\mathrm{p_f}}(\mathbf{r},t')U(\mathbf{r})\varphi_{\mathrm{p_i}}(\mathbf{r},t'). \end{aligned} \tag{9}$$

By taking the explicit form of the Volkov states (2) with the vector potential $A(t) = \boldsymbol{\epsilon}A_0\cos(\omega t)$ we observe that the A^2 term drops out from the transition matrix element (9), and T_{fi} becomes

$$\begin{aligned} T_{\mathrm{fi}} &= \sum_{n=-\infty}^{\infty} T^{(n)}_{\mathrm{fi}}, \\ T^{(n)}_{\mathrm{fi}} &= -2\pi i\delta\left(\frac{p_{\mathrm{f}}^2 - p_{\mathrm{i}}^2}{2m} + n\hbar\,\omega\right)J_n(z)\frac{U(\mathbf{q})}{(2\pi\hbar)^3}, \end{aligned} \tag{10}$$

before the time integration was done, the exponential expression was expanded into a Fourier series with the help of the Jacobi–Anger formula (Abramowitz & Stegun, 1972) which gave us the Bessel function

$$e^{iz\sin(\omega t)} = \sum_{n=-\infty}^{\infty} J_n(z)\,e^{in\omega t}. \tag{11}$$

The $U(\mathbf{q})$ is the Fourier transformed of the scattering potential with the momentum transfer of $\mathbf{q} \equiv \mathbf{p}_{\mathrm{i}} - \mathbf{p}_{\mathrm{f}}$ where $\mathbf{p}_{\mathrm{i}}$ is the initial and $\mathbf{p}_{\mathrm{f}}$ is the final proton momenta. The absolute value is $q = \sqrt{p_{\mathrm{i}}^2 + p_{\mathrm{f}}^2 - 2p_{\mathrm{i}}p_{\mathrm{f}}\cos(\theta_{p_{\mathrm{i}},p_{\mathrm{f}}})}$. In our case, for 49 MeV energy protons absorbing optical photons the following approximation is valid $q \approx 2p_{\mathrm{i}}|\sin(\theta/2)|$.

The Dirac delta describes photon absorptions ($n<0$) and emissions ($n>0$) with energy conservation.

$J_n(z)$ is the Bessel function with the argument of

$$z \equiv \frac{m_{\mathrm{e}}}{m_{\mathrm{p}}}a_0(\hat{\mathbf{q}}\boldsymbol{\epsilon})\frac{2p_i}{\hbar k_0}|\sin(\theta/2)|, \tag{12}$$

where m_{e} and m_{p} are the electron and proton masses, a_0 is the dimensionless intensity parameter (given above), $\hat{\mathbf{q}}$ and $\boldsymbol{\epsilon}$ are the unit vectors of the momentum transfer and the laser polarization direction. It can be shown with geometrical means that for low-energy photons where ($E_{\mathrm{ph}} < E_{\mathrm{p^+}}$) the angle in the scalar product of $\hat{\mathbf{q}}\boldsymbol{\epsilon} \equiv \cos\chi$ is $\chi = \pi/2 - \theta/2$ where θ is the scattering angle of the proton varying from 0 to π. See Figure 1.

From $(p_{\mathrm{i}}/\hbar k_0) = \sqrt{(m_{\mathrm{p}}/m_{\mathrm{e}})}\sqrt{(2m_{\mathrm{e}}c^2E_{\mathrm{i}}/\hbar^2\omega_0^2)}$ collecting the constants together the final formula for z reads

$$z = \frac{1.4166\times10^{-3}}{\hbar\,\omega_0}\sqrt{\frac{E_{\mathrm{p}}}{1836}}\sqrt{I}\times\cos(\chi)\times|\sin(\theta/2)|, \tag{13}$$

where the laser energy $\hbar\omega_0$ is measured in eV, the proton energy E_{p} in MeV, and the laser intensity I in W/cm^2 (note that this formula is valid for any kind of external laser field. For a 49 MeV proton projectile even the 10 keV X-ray laser has a negligible energy). The final differential cross-section formula for the laser associated collision with simultaneous nth-order photon absorption and emission processes is

$$\frac{d\sigma^{(n)}}{d\Omega} = \frac{p_f}{p_i} J_n^2(z) \frac{d\sigma_B}{d\Omega}. \tag{14}$$

The $d\sigma_B/d\Omega = (m/2\pi\hbar^2)^2 |U(\mathbf{q})|^2$ is the usual Born cross-section for the scattering on the potential $U(\mathbf{r})$ alone (without the laser field). The expression Eq. (14) was calculated with different authors using different methods (Bunkin & Fedorov, 1965; Bunkin *et al.*, 1973; Faisal, 1973; 1987; Kroll & Watson, 1973; Gontier & Rahman, 1974; Bergou, 1980; Bergou & Varró, 1980).

In our case the scattering interaction $U(\mathbf{r})$ is a central field $U(r)$ which is the sum of the Coulomb potential of a uniform charged sphere (Rudchik *et al.*, 2010) and a short range optical (Woods & Saxon, 1954) potential

$$U(r) = V_c(r) + V_{ws}(r) + i[W(r) + W_s(r)] + V_{ls}(r)\mathbf{l}\cdot\sigma, \tag{15}$$

where the Coulomb term is

$$V_c = \frac{Z_p Z_t e^2}{2R_0}\left(3 - \frac{r^2}{R_c^2}\right), \quad r < R_c,$$
$$V_c = \frac{Z_p Z_t e^2}{r}, \quad r \geq R_c, \tag{16}$$

where $R_c = r_0 A_t^{1/3}$ is the target radius calculated from the mass number of the target with $r_0 = 1.25$ fm. Z_p and Z_t are the charge of the projectile and the target and e is the elementary charge. This kind of regularized Coulomb potential helps us to avoid singular cross-sections and routinely used in nuclear physics.

The short-range nuclear part is given via

$$V_{ws}(r) = -V_r f_{ws}(r, R_0, a_0),$$
$$W(r) = -V_v f_{ws}(r, R_s, a_s),$$
$$W_s(r) = -W_s(-4a_s) f'_{ws}(r, R_s, a_s),$$
$$V_{ls}(r) = -(V_{so} + iW_{so})(-2) g_{ws}(r, R_{so}, a_{so}),$$
$$f_{ws}(r, R, a) = \frac{1}{1 + \exp\left(\frac{r-R}{a}\right)}, \tag{17}$$
$$f'_{ws}(r, R, a) = \frac{d}{dr} f_{ws}(r, R, a),$$
$$g_{ws}(r, R, a) = f'_{ws}(r, R, a)/r.$$

The constants V_r, W_v, V_{so}, and W_{so} are the strength parameters, and $a_{0,s,so}$, $R_{0,s,so}$ are the diffuseness and the radius parameters given for large number of nuclei. The f function is called the shape function of the interaction. As we will see at moderate collisions energies the complex terms become zero. In the last part of the present paper we will use the numerical parameters of Abdul-Jalil and Jackson (1979) for proton–carbon collision. According to the work of Hlophe *et al.* (2013) the complete analytic form of the Fourier transform of the WS potential can be calculated via the following kind of complex integrals $V(q) = \int_0^\infty dz\big((z\, exp(i\rho_k z))/(1 + exp(z - \alpha_k))\big)$, where $\rho_k = qa_k$, $\alpha_k = R_k/a_k$ and $z = r/a_k$ are dimensionless variables. The integrals can be evaluated by contour integration using the residuum theorem. For exhaustive details, see Hlophe *et al.* (2013). The Fourier transformed second term of Eq. (15) reads

$$V_{ws}(q) = \frac{V_r}{\pi^2}\left\{\frac{\pi a_0 e^{-\pi a_0 q}}{q(1 - e^{-2\pi a_0 q})^2}\left[R_0(1 - e^{-2\pi a_0 q})\cos(qR_0) - \pi a_0(1 + e^{-2\pi a_0 q})\sin(qR_0)\right] - a_0^3 e^{-(R_0/a_0)}\left[\frac{1}{(1 + a_0^2 q^2)^2} - \frac{2e^{-(R_0/a_0)}}{(4 + a_0^2 q^2)^2}\right]\right\}. \tag{18}$$

For the $W(q)$ imaginary term, the same expression was derived with W_v, a_s, and R_s instead of V_r, a_0, and R_0. The surface term W_s (r) [fourth term in Eq. (15)] gives the following formula in the momentum space:

$$W_s(q) = -4a_s\frac{W_s}{\pi^2}\left\{\frac{\pi a_s e^{-\pi a_s q}}{(1 - e^{-2\pi a_s q})^2}\left[(\pi a_s(1 + e^{-2\pi a_s q}) - \frac{1}{q}(1 - e^{-2\pi a_s q}))\cos(qR_s) + R_s(1 - e^{-2\pi a_s q})\sin(qR_s)\right] + a_s^2 e^{-(R_s/a_s)}\left[\frac{1}{(1 + a_s^2 q^2)^2} - \frac{4e^{-(R_s/a_s)}}{(4 + a_s^2 q^2)^2}\right]\right\}. \tag{19}$$

The last term in Eq. (15), the transformed spin–orbit coupling term leads to

$$V_{ls}(q) = -\frac{a_{so}}{\pi^2}(V_{so} + iW_{so})\left\{\frac{2\pi e^{-\pi a_{so} q}}{1 - e^{-2\pi a_{so} q}}\sin(qR_{so}) \times + e^{(-R_{so}/a_{so})}\left(\frac{1}{1 + a_{so}^2 q^2} - \frac{2e^{-R_{so}}}{4 + a_{so}^2 q^2}\right)\right\}. \tag{20}$$

where the momentum transfer is defined as above $\mathbf{q} \equiv \mathbf{p_i} - \mathbf{p_f}$. The low-energy transfer approximation formula $q \approx 2p_i \cdot |\sin(\theta/2)|$ is valid.

The Fourier transform of the charged sphere Coulomb field is also far from being trivial

$$V_c(q) = \frac{Z_p Z_t e^2}{2^{(5/6)}\sqrt{\pi} q^3}\left(-2\cdot 3^{(1/3)} q \cos[2^{(2/3)}3^{(1/3)}q] + 2^{(1/3)}(1 + 2\cdot 2^{(1/3)}3^{(2/3)}q^2)\sin[2^{(2/3)}3^{(1/3)}q]\right) + 3Z_p Z_t e^2\sqrt{\frac{2}{\pi}}\left(\frac{i\pi|q|}{2q} - \mathrm{Ci}[2^{(2/3)}3^{(1/3)}q] + \log(q) - \log|q| - i\mathrm{Si}[2^{(2/3)}3^{(1/3)}q]\right), \tag{21}$$

where Ci and Si are the cosine and the sine integral functions, respectively; for details see Abramowitz and Stegun (1972).

3. RESULTS

We applied the outlined method to 49 MeV proton–^{12}C scattering. Table 1 contains the parameters of the used Woods–Saxon potential.

Note that the complex part W_v and the complex part of the spin–orbit term W_{so} are zero at this energy.

Figure 2 presents the angular differential cross-section in the first Born approximation of the various Woods–Saxon potential terms for 49 MeV elastic proton–^{12}C scattering. The different lines represent the different terms Eqs. (18)–(20). The laboratory frame is used in the calculation. For a better transparency the contributions of the regularized Coulomb term is not presented. Our calculated total cross-section of the elastic scattering is 201 mbarn which is consistent with the data of Abdul-Jalil and Jackson (1979).

In our case, the laser photon energy is $\hbar\omega_0 = 1.56$ eV, which means 800 nm wavelength and the proton energy is $E_p = 49$ MeV. With these values the argument of the Bessel function Eq. (13) becomes the following:

$$z = 1.48 \times 10^{-3}\sqrt{I} \times \cos(\chi) \times |\sin(\theta/2)| = \mathrm{I} \times \cos(\chi) \times |\sin(\theta/2)|. \tag{22}$$

Figure 3 shows the angular differential cross-section for $n = 0, 1, 2$ photon absorptions for $\mathcal{I} = 100$ which means $I = 4.56 \times 10^{11}$ W/cm^2 moderate intensity. Note that the cross-sections for single and double photon absorption are almost the same. The single-photon absorption total cross-section is 0.5 mbarn.

For large laser field intensities, which means large z arguments of the Bessel functions the following asymptotic expansion can be used for a fixed index (Abramowitz & Stegun, 1972)

$$J_n(z) = \sqrt{2/(\pi z)}\cos(z - n\pi/2 - \pi/4), \tag{23}$$

which means an approximate $1/\sqrt{\sin(\theta)\cos(\theta)}$ angle dependence which has a strong decay for large scattering angles. Note that even this function shows very rapid oscillations.

Table 1. Parameters of the applied potential for proton–^{12}C collision at $E_i = 49$ MeV

Name of the parameter	Numerical value
V_R	31.31 (MeV)
R_0	1.276 (fm)
a_0	0.68 (fm)
W_s	5.98 (MeV)
r_s	0.890 (fm)
a_s	0.586 (fm)
V_{so}	2.79 (MeV)
R_{so}	0.716 (fm)
a_{so}	0.222 (fm)

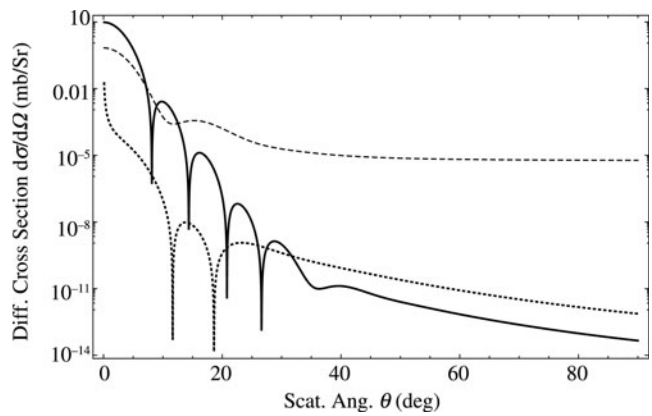

Fig. 2. The angular differential cross-sections in the first Born approximation of the various Woods–Saxon potentials terms for 49 MeV elastic proton–^{12}C scattering. The solid, dashed, and dotted lines are the contributions of Eqs. (18, 19, 20), respectively. Note the different smoothness and different back scattering values of the different terms.

Figure 4 shows the same kind of cross-sections for $z =$ 10,000 (which means $I = 4.56 \times 10^{15}$ W/cm^2 intensity) and for $z = 6.61 \times 10^6$ (which means $I = 2.0 \times 10^{21}$ W/cm^2 intensity), respectively. Only the $n = 1$ one photon absorption process is considered.

As a second physically relevant example we present the scattering cross-sections in the presence of an X-ray laser field. For the 10 keV laser field of 10^{16} W/cm^2 intensity the I parameter in Eq. (22) has the values of 0.162. Figure 5 presents the cross-sections curves for $n = 0, 1, 2$. Note that the I parameter makes the Bessel functions very small at small angles.

4. SUMMARY

We presented a formalism which gives an analytic angular differential cross-section model for laser-assisted proton

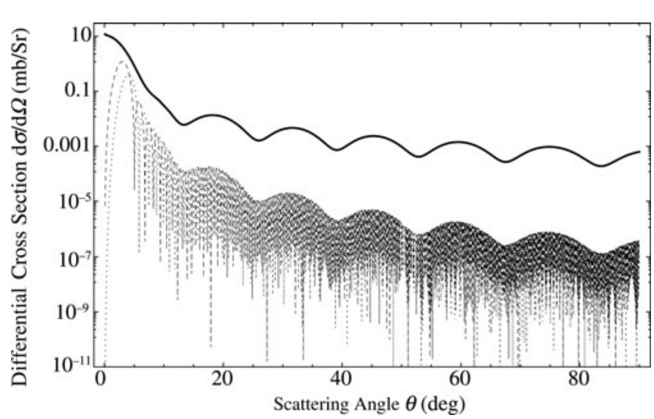

Fig. 3. The calculated angular differential cross-sections from Eq. (14) for $I = 4.56 \times 10^{11}$ W/cm^2 laser field intensity ($\mathcal{I} = 100$). The thick solid, thin long-dashed, and thin short-dashed lines are for $n = 0,1,2$ photon absorptions.

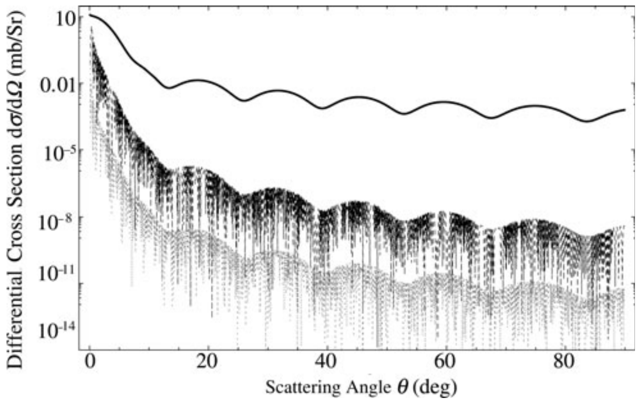

Fig. 4. Comparison of the calculated angular differential Born cross-sections to two laser-assisted cross-sections with a single-photon absorption at high photon intensities. The black thick line represents the Born cross-section, the black thin solid line is for $I = 4.56 \times 10^{15}$ W/cm^2 intensity ($\mathcal{I}$ = 10,000). The dashed gray line is close to the relativistic threshold with $I = 2.0 \times 10^{21}$ W/cm^2 laser field intensity ($\mathcal{I} = 6.61 \times 10^6$).

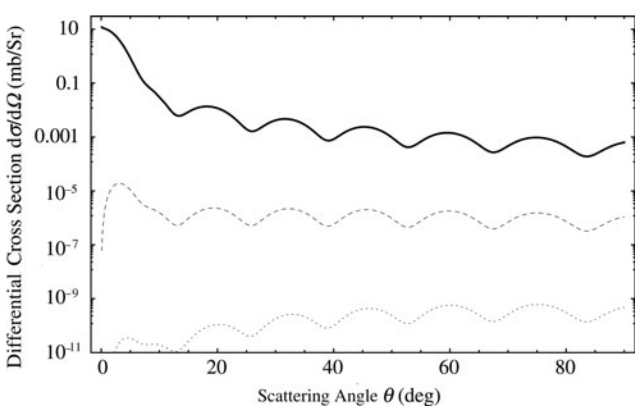

Fig. 5. The calculated angular differential cross-sections for a 10^{16} W/cm^2 intensity 10 keV X-ray laser beam. The thick solid, thin long-dashed, and thin short-dashed lines are for n = 0,1,2 photon absorptions, respectively.

nucleon scattering on a Woods–Saxon optical potential where the nth-order photon absorption is taken into account simultaneously. We coupled the mathematical description of multi-photon processes to the well-established low-energy nuclear physics description. As an example the physically relevant proton–^{12}Ca collision system was investigated at moderate 49 MeV proton energies. Two different kinds of laser fields are investigated. The first one is the optical Ti:sapphire system with wavelength of 800 nm with intensities in the range of 10^{11}–10^{21} W/cm^2. As a second system we took a 10 keV X-ray laser field with 10^{16} W/cm^2 intensity. The calculated cross-sections are much lower than the elastic cross-sections in all cases. We hope that our study will give a strong impetus and couple the nuclear and laser physics community together to perform such experiments in the ELI or X-FEL facilities which will be available in a couple of years.

ACKNOWLEDGMENTS

We thank for Professor Gyula Bencze for useful discussions and comments. S. V. has been supported by the National Scientific Research Foundation OTKA, Grant No. K 104260. Partial support by the ELI-ALPS project is also acknowledged. The ELI-ALPS project (GOP-1.1.1-12/B-2012-0001) is supported by the European Union and co-financed by the European Regional Development Fund.

REFERENCES

Abdul-Jalil, I. & Jackson, D.F. (1979). Energy dependence of the optical potential for proton scattering from light nuclei. *J. Phys. G: Nucl. Phys.* **5**, 1699.

Abramowitz, M. & Stegun, I.A. (1972). *Handbook of Mathematical Functions*, chap. 9, p. 364. 10 edn. Applied Mathematics Series, Washington, D.C.: U.S. Government Printing Office.

Barna, I.F., Apagyi, B. & Scheid, W. (2000). Localization of non-local potentials by a Taylor expansion method. *J. Phys. G: Nucl. Phys.* **26**, 323–331.

Bergou, J. (1980). Wavefunctions of a free electron in an external field and their application in intense field interactions. I. Non-relativistic treatment. *J. Phys A: Math. Gen.* **13**, 2817–2822.

Bergou, J. & Varró, S. (1980). Wave functions of a free electron in an external field and their application in intense field interactions, II. Relativistic treatment. *J. Phys. A: Math. Gen.* **13**, 2823–2837.

Bunkin, F.V. & Fedorov, M.V. (1965). Bremsstrahlung in a strong radiation field. *Zh. Eksp. Teor. Fiz.* **49**, 1215–1221.

Bunkin, F.V., Kazakov, A.E. & Fedorov, M.V. (1973). Interaction of intense optical radiation with free electrons (nonrelativistic case). *Usp. Fiz. Nauk.* **15**, 416–435.

Di Piazza, A., Müller, C., Hatsagortsyan, K.Z. & Keitel, C.H. (2012). Extremely high-intensity laser interactions with fundamental quantum systems. *Rev. Mod. Phys.* **84**, 1177–1228.

Ehlotzky, F., Jaron, A. & Kaminski, J. (1998). Electron–atom collisions in a laser field. *Phys. Rep.* **297**, 63–153.

Faisal, F.H.M. (1973). Collision of electrons with laser photons in a background potential. *J. Phys. B: At. Mol. Phys.* **6**, L312–L315.

Faisal, F.H.M. (1987). *Theory of Multiphoton Processes*. New York: Plenum Press.

Gontier, Y. & Rahman, N. (1974). Intense electromagnetic field and multiphoton processes. *Lett. al Nuovo Cim.* **9**, 537–540.

Greiner, W. & Maruhn, J.A. (1996). *Nuclear Models*. Heidelberg, Germany: Springer-Verlag.

Gunst, J., Litvinov, Y.A., Keitel, C.H. & Pálffy, A. (2014). Dominant secondary nuclear photoexcitation with the X-ray free-electron laser. *Phys. Rev. Lett.* **112**, 082501 (pages 5).

Habs, D., Tajima, T., Schreiber, J., Barty, C.P.J., Fujiwara, M. & Thirolf, P.G. (2009). Vision of nuclear physics with photo-nuclear reactions by laser-driven beams. *Eur. Phys. J. D* **55**, 279–285.

Hlophe, L., Elster, C., Johnson, R.C., Upadhyay, N.J., Nunes, F.M., Arbanas, G., Eremenko, V., Escher, J.E. & Thompson, I.J. (TORUS Collaboration) (2013). Separable representation of phenomenological optical potentials of Woods-Saxon type. *Phys. Rev. C* **88**, 064608, (pages 11).

Hodgson, P.E. (1994). *The Nucleon Optical Model*. Singapore: World Scientific Co. Pvt. Ltd.

Kornev, A.S. & Zon, B.A. (2007). Nuclear excitation by the atomic electron rescattering in a laser field. *Laser Phys. Lett.* **4**, 588.

KROLL, N.M. & WATSON, K.M. (1973). Charged-particle scattering in the presence of a strong electromagnetic wave. *Phys. Rev. A* **8**, 804–809.

LEDINGHAM, K.W.D. (2005). Laser induced nuclear physics and applications. *Nucl. Phys. A* **752**, 633–644.

PAHLAVANI, M.R. & MORAD, R. (2010). Validity of born approximation for nuclear scattering in path integral representation. *Adv. Stud. Theor. Phys.*, **4**, 393–404.

RUDCHIK, A., SHYRMA, Y., KEMPER, K., RUSEK, K., KOSHCHY, E., KLICZEWSKI, S., NOVATSKY, B., PONKRATENKO, O., PIASECKI, E., ROMANYSHYNA, G., STEPANENKO, Y., STROJEK, I., SAKUTA, S., BUDZANOWSKI, A., GŁOWACKA, L., SKWIRCZYŃSKA, I., SIUDAK, R., CHOIŃSKI, J. & SZCZUREK, A. (2010). Isotopic effects in elastic and inelastic 12C + 16, 18O scattering. *Eur. Phys. J. A* **44**, 221–231.

VARNER, R., THOMPSON, W., MCABEE, T., LUDWIG, E. & CLEGG, T. (1991). A global nucleon optical model potential. *Phys. Rep.* **201**, 57–119.

von Geramb, H.V. Ed. (1979). *Microscopic Optical Potentials, Lecture Notes in Physics*. Vol. 89, Hamburg Topical Workshop on Nuclear Physics, Heidelberg, Germany: Springer-Verlag Berlin Heidelberg.

WOODS, R.D. & SAXON, D.S. (1954). Diffuse surface optical model for nucleon-nuclei scattering. *Phys. Rev.* **95**, 577–578.